Pt-MWCNTs as electrocatlyst for Oxidation of *p*-methoxytoluene (*p*-MT) to *p*-methoxybenzaldehyde (*p*-MeOBA)

Yanmei Liao, Yinghong Zhu[*]*, Lianbang Wang*

College of chemical Engineering, Zhejiang University of Technology, Hangzhou, 310023 Zhejiang China
[*]E-mail: yhzhuchem@zjut.edu.cn

Electrochemical synthesis is promising for the new processes focused on the improvement of electrochemical oxidation occurring on the electrodes. Herein, we report a facile preparation method of Pt nanoparticles being highly dispersed on multi-walled carbon nanotubes (MWCNTs). The morphology of the prepared electrode material Pt-MWCNTs was measured by X-ray diffraction (XRD), Transmission electron microscopy (TEM) and X-ray Photoelectron Spectroscopy (XPS). These results demonstrated that the Pt nanoparticle of Pt-MWCNTs has face-centered cubic (fcc) structure typical and was highly dispersed on MWCNTs (marked as Pt-MWCNTs). The activity and stability of the Pt-MWCNTs electrode was characterized by Cyclic voltammetry (CV) and the controlled-potential electrolysis. The results showed that the Pt-MWCNTs exhibited excellent activity and stability on the electrochemical oxidation for *p*-methoxytoluene (*p*-MT) to *p*-methoxybenzaldehyde (*p*-MeOBA) in aqueous solution at 40 ℃.

1. INTRODUCTION

Through the oxidation of the methyl group could lead successfully to aromatic alcohol, aromatic aldehyde and aromatic acid. Among them, aromatic aldehydes have many applications using as the key intermediates of specialty chemicals, soaps, detergents, perfumes, insect attractants, drug synthesis [1-4]. Aliphatic aldehydes can be easily produced by numerous, mainly catalytic oxidation processes with high yield. While, oxidation of C-H bonds of aromatics to aldehydes is usually occuring need high temperatures, acidic or basic conditions, and even strong oxidants or reductants [5-8].

The electrochemical oxidation of aromatic C-H bonds to aromatic aldehydes is an important method. As a result, many groups have focused on oxidative of *p*-MT including indirect or direct electrochemical oxidation [9-14]. Jiang et al [15] reported that electrochemical oxidation of *p*-MT on the

graphite/Nafion membrane composite electrode in acetonitrile, the products were *p*-MeOBA and *p*-methoxybenzoic acid (*p*-MeOBAc). Said et al [16] reported that used platinum (Pt) as working oxidation of *p*-MT, when adding water to the acetic acid can increases the yield of *p*-MeOBA. Falgayrac et al [17] used graphite electrode oxidative of *p*-MT in acetic acid solution founded that in the presence of water, there were can oxidation to *p*-MeOBA and eventually to *p*-MeOBAc. Bejan et al [18] oxidation of *p*-MT in solution in acetic acid on graphite electrode with oxygen conditions the yields of *p*-MeOBA higher than 80%. Bystron et al [19] reported the electrochemical oxidation of *p*-MT in ionic liquid (IL) using the glassy carbon electrode as working electrode. Furthermore, Zhu et al [20] have been reported that using a Pt foil as work electrode, electrochemical oxidation of *p*-MT to *p*-MeOBA in IL at room temperature. In order to reduce the amount of IL, Zhu et al [21] prepared the IL and MWCNTs composite as work electrode or supporting electrolyte, which presented excellent electrochemical performance, and the yield of *p*- MeOBA outperforms 85% at 60 ℃. However, the development anodic oxidation of the methyl group of toluene leads successively to formation aromatic aldehydes there are still many problems (such as Pt electrode is very expensive, low selectively even excessive oxidation to acid and so on) restricting the practical application of electrochemical oxidation.

Generally, the size of Pt particles and dispersion on supporting materials can influence the activity of electrode materials [22]. MWCNTs owing to their diversified constructions, high chemical stability, high electrical conductivity, and large active surface area, have been were widely utilized as electrocatalyst supports [23]. Therefore, herein we reported a nano Pt-MWCNs and used as work electrode towards the electrochemical oxidation of *p*-MT to *p*-MeOBA.

2. EXPERIMENTAL

2.1. Materials

LiClO$_4$, acetone, ethanol, acetonitrile (CH$_3$CN), H$_2$PtCl$_6$·6H$_2$O, *p*-MT, *p*-methoxybenzyl and *p*-methoxy-4-propylbenzene, Nafion (5wt.%) were purchased from Sigma-Aldrich (China), and nitric acid (HNO$_3$), methanol (MeOH), tetrahydrofuran (THF), N,N-dimethylformamide (DMF), dichloromethane (CH$_2$Cl$_2$) were purchased from Sinopharm Chemical Reagent Co. Ltd (China). 2-methylanisole, 3-methylanisole and *p*-chlorotuluene were purchased from Xiyashiji Co. Ltd (China). Carbon paper (CP) was purchased from Shanghai Hesen Electric Co. Ltd. MWCNTs (97%, 40-60 nm in diameter) were purchased from Shenzhen Nanotech. Prot. Co. Ltd. (China). Glass Carbon (GC, Φ=5mm) electrode, alumina powder (50nm, 500nm) were purchased from Tianjin Aida Co. Ltd. The H$_2$/Ar gas purify is 99.999%). The water was purified by a Millipore system. All the reagents were analytical grade without further purification.

2.2 Electrocatalyst preparation

MWCNTs were treated in 65% HNO$_3$ solution for 4 h at 150 ℃, then they were filtered and washed with deionized water until the filtrate aqueous tested as neutral, then dried in oven at 80 ℃ for

12 h before use. MWCNTs-supported Pt (10 wt.%) catalyst was prepared by incipient wetness impregnation method using appropriate amounts of aqueous solution of $H_2PtCl_6 \cdot 6H_2O$. The sample were calcined at 500 ºC for 2 h under 5% H_2/Ar flow (100 mL min-1) at the ration of 5 ºC min^{-1}.

2.3 Electrode modification

The GC electrode and Pt electrode were polished carefully with alumina powder 500 nm and 50 nm on a soft polishing cloth (Buehler). After sonicated in acetone, they were thoroughly rinsed with deionized water to obtain a clean renewed electrode surface and dried at room temperature for use.10 mg of electrocatalyst was dispersed into 700 μL of ethanol and 250 μL of distilled water and 50 μL of Nafion solution (5 wt.%) were combined to form a slurry. This suspension was treated under ultrasonic condition for 1 h. Finally, 10 μL of the suspension was placed on the surface of the GC surface and dried at room temperature (the electrode was denoted as Pt-MWCNTs/GC). In addition, 150 μL of the slurry was added dropwise onto CP electrode (1 cm×1 cm) and dried at room temperature for 12 h (the electrodes were denoted as Pt-MWCNTs/CP). After electrolysis, the Pt-MWCNTs/CP electrode was washed with ethanol and deionized water, dried at room temperature for reuse.

2.4 Characterizations

The phase purity of the as-synthesized sample was analyzed by XRD patterns with a RIGAKU Ultimate IV diffractometer using Cu Kα radiation. TEM was obtained by using JEM-2010Ex (Japan) with an accelerating voltage of 200 kV. Specs spectrometer was used for XPS measurements with Thermo Scientific K-Alpha+ and C 1s line at 284.8 eV was chosen as a reference point. All XPS peaks were fitted using a Gaussian function. The pH of the various electrolysis systems was measured with a PHS-3C acidometer (Shanghai REX, China) at room temperature. The major products were detected using GC-MS (Thermo Fisher). The yields (Y) and selectivity (S) were detected by GC-MS analysis.

2.5 Electrochemical measurements

CV was tested using a CHI 660D (Shanghai Chenhua) electrochemical workstation. The modified Pt-MWCNTs/GC electrode (or GC electrode) was used as the working electrode (WE), a 2 cm × 2 cm Pt foil as the counter electrode (CE), and a platinum wire (0.5 mm diameter) electrode as the reference electrode (RE). The CV measurement were performed at room temperature. The controlled-potential electrolysis was carried out in a 20 mL undivided electrochemical cell and the total solvent was 10 mL The Pt-MWCNTs/CP electrode (1 cm×1 cm) was used as the working electrode, a 2 cm × 2 cm Pt foil as the counter electrode, and a Pt wire (0.5 mm diameter) electrode as the reference electrode. The concentration of all used aromatic substrate were 0.04 M and the electrolysis potential at 1.5/1.8 V. All the electrolysis experiments were carried out at 25-40 ºC for 6 h under the solution stirred with a magnetic stirrer. 0.2 M $LiClO_4$ was used as the supporting electrolyte in the solution.

3. RESULTS AND DISCUSSION

3.1. Characterization of Pt-MWCNTs

Fig.1a shows the XRD patterns of MWCNTs and Pt-MWCNTs samples. For the MWCNTs, a strong peak at $2\theta=26.3°$ and two weak peaks at $2\theta=42.9°$ and $54.5°$ were observed, corresponding to the (002), (100) and (004) diffraction patterns of typical graphitized (JCPDS: 41-1487). The 2θ of 39.9, 46.1, and 67.4° are assigned to (111), (200), and (220) crystalline plane diffraction peaks, respectively, indicating the fcc crystal structure typical of Pt was successfully deposited on MWCNTs. The structure and morphology of the Pt-MWCNTs was by TEM, as shown in Fig.1b and Fig.1d. It was found that the Pt nanoparticles were homogeneous distribution on the MWCNTs and the average Pt nanoparticles size was calculated to be about 1.30 nm. Moreover, the crystal structure of Pt nanoparticles was measured by high resolution TEM image as shown in Fig.1c, and the lattice fringe distance corresponding to Pt (111) is calculated to be 0.23 nm, which was found to agree with in the literature reported [24].
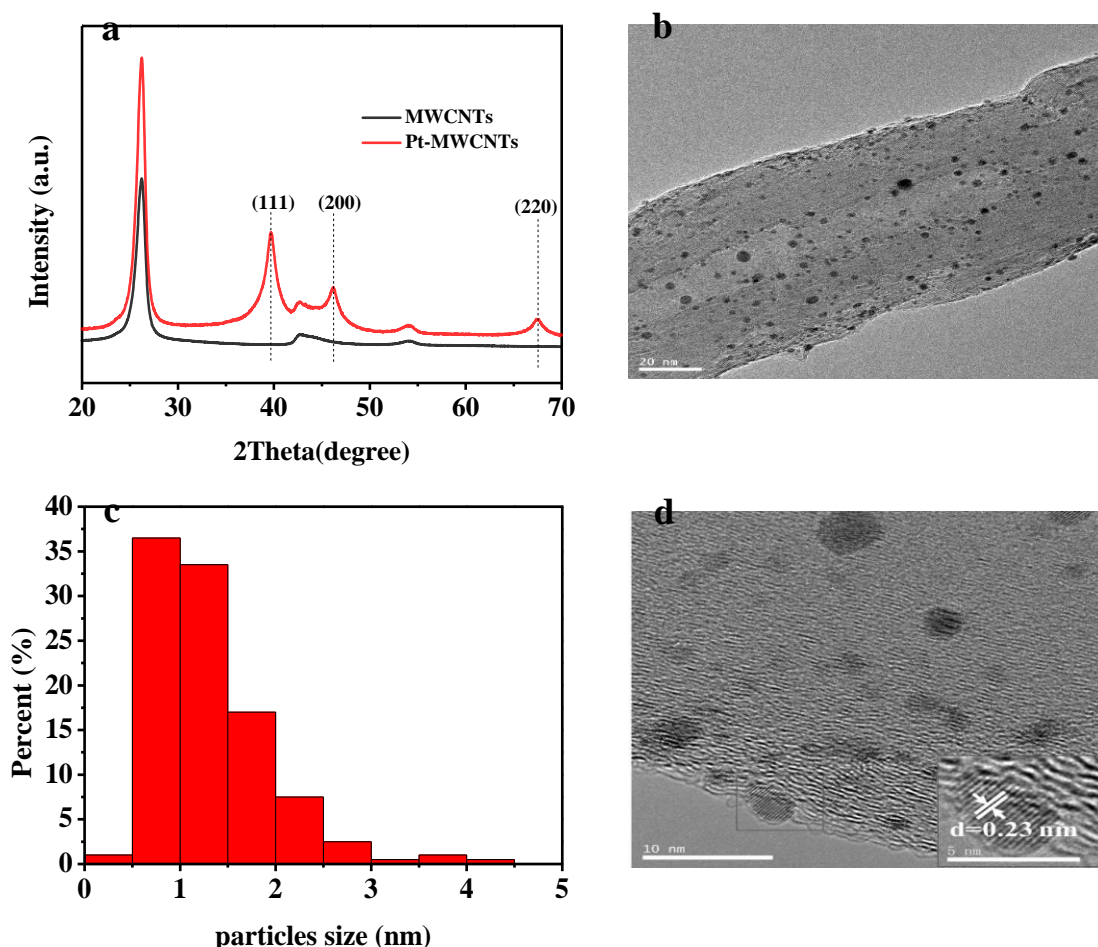
Figure 1. The XRD pattern of MWCNTs and Pt-MWCNTs samples(a); TEM images (b and d) of Pt-MWCNTs sample and the Pt particle size distribution (c).

Fig.2a shows the survey X-ray Photoelectron Spectroscopy (XPS) spectrum of Pt-MWCNTs sample, the main peaks observed are C 1s, O 1s and Pt 4f peaks. Fig.2b shows the XPS spectral of the Pt 4f and two pairs of peaks were observed in Pt4f region. The ratio of $4f_{7/2}$ /$4f_{5/2}$ signals was found to be 4/3, which is agreed with the former study values in the literature [24-25]. The most intense doublet (71.8 and 75.1 eV) is attributed to Pt(0). The second set of doublets (72.8 and 76.7eV) can be assigned to the Pt(II), due to the incomplete reduction platinum from (H_2PtCl_6) precursor [26].
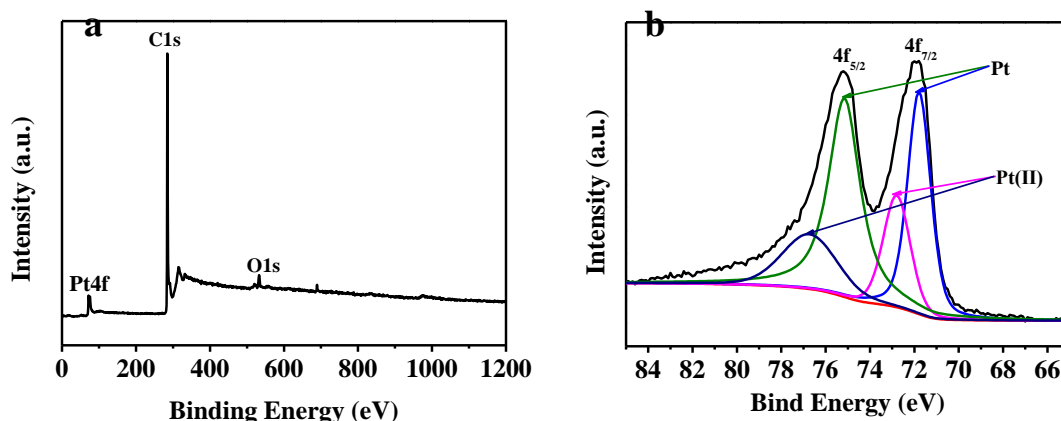
Figure 2. XPS of the Pt-MWCNTs survey spectrum (a) and Curve-fitted of Pt 4f (b).

3.2. Electrochemical Performance
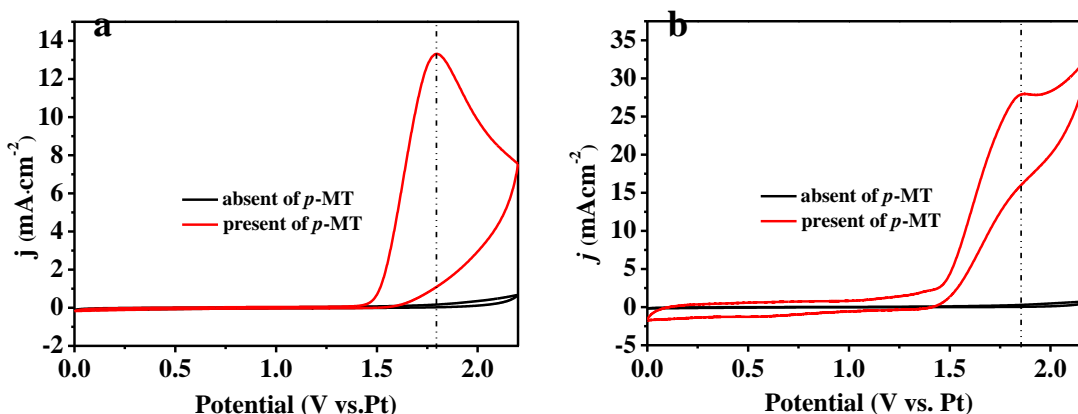
Figure 3. The cyclic voltammograms of *p*-MT on GC electrode (a) and Pt-MWCNTs/GC electrode (b) at scan rate of 50 mV s^{-1} at room temperature ($c_{(p\text{-}MT)}$= 0.04 M).

To investigate the feasibility of the approach outlined above, we chose *p*-MT as a model substrate by CV in 0.2 M LiClO$_4$ as supporting electrolyte. Fig.3 shows the electrochemical response of *p*-MT on the Pt-MWCNTs/GC electrode and GC electrode in acetonitrile-water (9:1) (black line) at 50 mV s^{-1} of scan rate at room temperature. From the CV curves, apparent oxidation peaks were exhibited on GC and

Pt-MWCNTs/GC electrodes, respectively, while no reduction peaks were found. For the GC electrode, the current density of 13.38 mA cm^{-2} was observed when the oxidation of *p*-MT at 1.80 V, while the current density was 27.94 mA cm^{-2} on the Pt-MWCNTs/GC electrode at 1.86 V. The higher oxidation peak current density and oxidation peak potential of the Pt-MWCNTs/GC electrode than that of the GC electrode, is reasonably attributable to the electrocatalytic activity of the nano Pt-MWCNTs.

Attempts to optimize the reaction conditions, the results of controlled-potential electrolysis in an undivided electrochemical cell at different conditions were shown in Table 1. The yields of *p*-MeOBA was shifted from trace to 25% in different solvents (entries 1~7). Also, the yields of *p*-MeOBA was greatly depended on the temperature (entries 7~10) and the electrode materials (entries 10~13) As a result, the yield of *p*-MeOBA reached to 91% at the Pt-MWCNTs/CP electrode at 40 °C in CH$_3$CN-H$_2$O (9:1) aqueous solution. Also, the pH and conductivity (δ) of solutions of 0.2 M LiClO$_4$ at room temperature were measured (Table 2). So that we assumed that the best potential electrolysis condition is in acetonitrile-water (9:1) solution at 40 ℃.
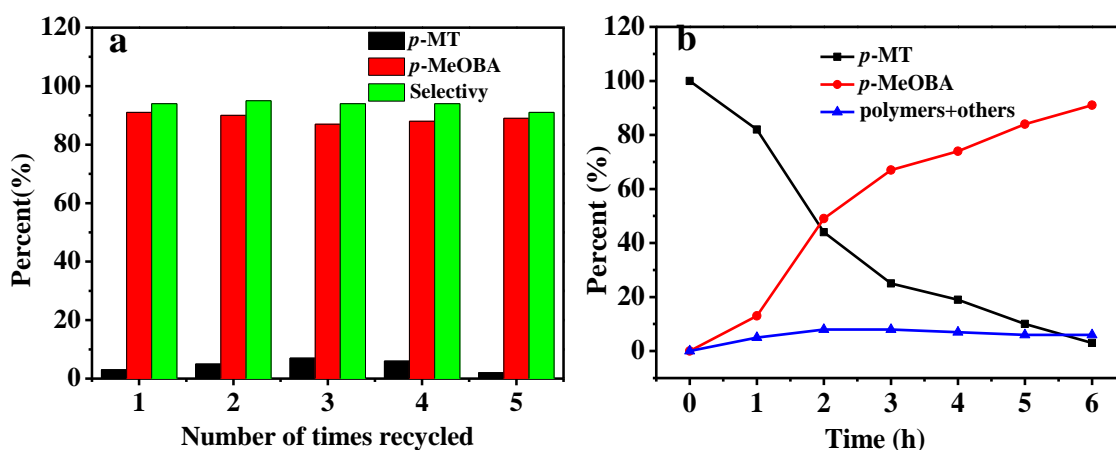
Figure 4. Recycling use of the Pt-MWCNTs/CP electrode in the electrochemical oxidation of *p*-MT (a) and the curves of products on different electrolysis time (b).
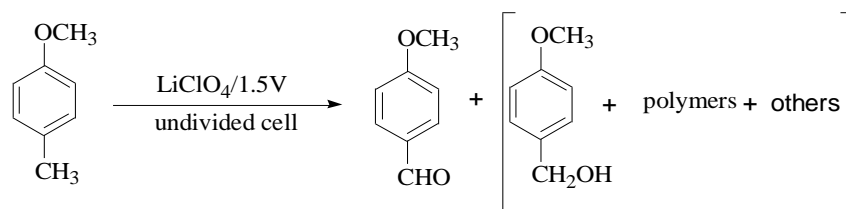
The results of different substrates with methyl-substituted aromatics for controlled-potential electrolysis under the optimized reaction conditions were shown in Table 3. It was obvious that *p*-substituted substrates with higher yield and selectivity than ortho or meta-substituted (entries 1-3), suggested that the *p*-MT is relatively easy to oxidize due to the electron donor effect of the methoxygroup. Also, we noted that electron donating substrate (entry 1, 6 and 7) easier to oxidize than

electron absorption substrate, there were no products were detected in entry 4 and 5. Obviously, Pt-MWCNTs/CP exhibited higher yield of *p*-MeOBA than most reported electrocatalysts, including graphite [6], Pt [20-21]and CoMn$_2$O$_4$/titanium [28]. The more detailed comparisons are displayed in Table 4. To understand the Pt-MWCNTs/CP electrocatalyst enhanced the yield of *p*-MeOBA, maybe the functionalized MWCNTs support ensures the Pt nanoparticles are highly monodispersed and it also provides high density of active sites on the Pt nanoparticles, which has the benefit of improving the catalytic activity and selectivity for C-H bands oxidation reaction [23,30]. Also, the suitable proportion of water can enhance the yield of *p*-MeOBA [6].

Table 1. The Controlled-potential electrolysis of *p*-MT at different reaction condition.

Entry	Work electrode (1×1cm^2)	Solvent	Temp.	yield (%)	Selectivity (%)
1	Pt-MWCNTs/CP	CH$_3$CN	25	4	17
2	Pt-MWCNTs/CP	H$_2$O	25	5	58
3	Pt-MWCNTs/CP	MeOH	25	7	40
4	Pt-MWCNTs/CP	THF	25	trace	trace
5	Pt-MWCNTs/CP	DMF	25	trace	trace
6	Pt-MWCNTs/CP	CH$_2$Cl$_2$	25	trace	trace
7	Pt-MWCNTs/CP	CH$_3$CN-H$_2$O (9:1)	25	25	33
8	Pt-MWCNTs/CP	CH$_3$CN-H$_2$O (5:5)	25	16	25
9	Pt-MWCNTs/CP	CH$_3$CN-H$_2$O (9:1)	30	52	74
10	Pt-MWCNTs/CP	CH$_3$CN-H$_2$O (9:1)	40	91	94
11	CP	CH$_3$CN-H$_2$O (9:1)	40	17	28
12	MWCNTs/CP	CH$_3$CN-H$_2$O (9:1)	40	21	31
13	Pt foil	CH$_3$CN-H$_2$O (9:1)	40	9	11

Table 2. The pH and conductivity (δ) of 0.2 M LiClO$_4$ in different solvent

Solution	pH	δ (mS cm^{-1})
CH$_3$CN	4.9	16.72
H$_2$O	7.3	17.41
THF	4.8	0.98
DMF	6.4	8.61
CH$_2$Cl$_2$	1.7	0.03
MeOH	6.5	8.53
CH$_3$CN-H$_2$O (9:1)	6.3	18.85
CH$_3$CN-H$_2$O (5:5)	6.9	16.61

Durability and stability are also important factors to evaluate the electrochemical performance of the electrode materials. The Pt-MWCNTs/CP electrode was reused for 5 times and the electrolysis results were shown in Fig.4a. The yield of the major product *p*-MeOBA decreased slowly in the 5 times reused results, the of major product *p*-MBA decrease very slowly, relatively. It suggested that the recycled electrode exhibited excellent electrochemical activity for the electrooxidation of *p*-MT.

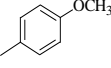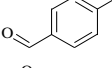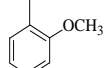**Table 3.** The Controlled-potential electrolysis of different aromatic compounds (C *substrate*=0.04 M).

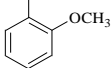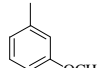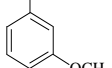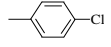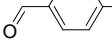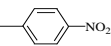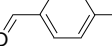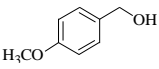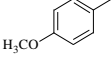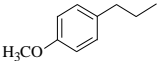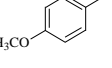| Entry	Substrate	E_{ox} (V)	Major Product	Major Product (Y/%)	Major Product (S/%)
1		1.5		91	94
2		1.5		8	30
3		1.5		trace	trace
4		1.5		trace	trace
5		1.5		trace	trace
6		1.5		>99	> 99
7		1.8		93	> 99

Table 4 Comparison of various electrocatalyst for *p*-MT oxidation performance to our Pt-MWCNTs/CP
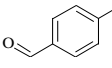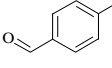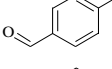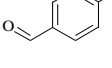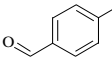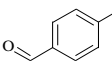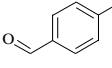
Catalyst	Solvent	Major Product	Y(S)	Ref.
Pt-MWCNTs/CP	0.2M LiClO$_4$/CH$_3$CN-H$_2$O (9:1)		91	This work
graphite	acetic acid-H$_2$O (9:1)		70	6
Pt	EmiAc/MWCNTs/H$_2$O		87	20
Pt	3.1M EMIMBF$_4$/H$_2$O		90	21
graphite	1M NaOAC/acetic acid		36.9	27
CoMn$_2$O$_4$/titanium	1M H$_2$SO$_4$/5MH$_2$O/MeOH		60(S)	28
Titanium	Ce(IV)/1M H$_2$SO$_4$		~80	29

Fig.4b shows the controlled-potential electrolysis performance of *p*-MT on the Pt-MWCNTs/CP. The yield of *p*-MeOBA increased greatly at the first 2 hours, and reaches to a high yield of 91% after 6 hours. During the process, there was at most 8% polymers and others were detected. All the results showed the excellent catalytic activity of Pt-MWCNTs/CP for oxidation of a C-H to a carbonyl unit.

4. CONCLUSIONS

In summary, high activity and stability for Pt-MWCNTs/CP electrode has been experimentally proven towards electrochemical oxidation of *p*-MT in acetonitrile-water (9:1) solution. Undoubtedly, electrochemical oxidation C-H bonds should be potential in organic synthesis. In the future, we will devote to synthesis electrode materials for widely C-H bonds electrochemical oxidation.

References

1. B.M. Reddy, M.V. Kumar and K.J. Ratnam, *Appl. Catal. A: Gen.*, 181 (1999) 77.
2. A. Martin, U. Bentrup and G.U. Wolf, *Appl. Catal. A: Gen.*, 227 (2002) 131.
3. D. Rubio, D. Zantte, F. Nome and C.A. Bunton, *Langmuir*, 10 (1994) 1155.
4. P. Lątka, T. Berniak, M. Drozdek, W. Ewa and P. Kustrowski, *Catal. Commun.*, 115 (2018) 73.
5. M. Moselage, J. Li and L. Ackermann, *ACS Catal.*, 2016 (6) 498.
6. U. Bentrup, A. Martin and G.U. Wolf, *Catal. Today*, 78 (2003) 229.
7. K. Kornela, O. Beata, E. Witek, P. Latka, J. Zawadiak and L. Proniewicz, *Catal. Lett.*, 145 (2015) 1856.
8. A.S. Larsen, K. Wang, M.A. Lockwood, G.L. Rice, T.J. Won, S. Lovell, M. Sadilek, F. Turecek and J.M. Mayer, *J. Am. Chem. Soc.*, 124 (2002) 10112.
9. V. Devadoss, C.A. Basha and K. Jayaraman, *Ind. Eng. Chem. Res.*, 47 (2008) 4607.
10. T. Tzenakis and A. Savall, *J. Appl. Electrochem.*, 27 (1997) 589.
11. E. Lodowicks and F. Beck, *J. Appl. Electrochem.*, 1998 (28) 873.
12. A. ViniPriya, A. J. Bosco, T. Maiyalagan, N. Xavier and D. Vasudevan, *Int. J. Electrochem. Sci.*, 21 (2017) 1272.
13. T. Bystron, Z. Hasnik and K. Bouzek, *J. Electrochem. Soc.*, 156 (2009) 179.
14. A. Attour, S. Rode, A. Ziogas, M. Matlosz and F. Lapicque, *J. Appl. Electrochem.*, 38 (2008) 339.
15. J. Jiang, B. Wu and C. Cha, *Electrochim. Acta*, 43 (1998) 2549.
16. A.H. Said, M. Mhalla, C. Amatore and J. N. Verpeaux, *J. Electroanal. Chem.*, 464 (1999) 85.
17. G. Falgayrac and A. Savall, *J. Appl. Electrochem.*, 28 (1998) 1137.
18. D. Bejan and A. Savall, *J. Electroanal. Chem.*, 2001 (507) 234.
19. T. Bystron and K. Bouzek, *J. Electrochem. Soc.*, 160 (2013) 117.
20. Y. Zhu, Y. Zhu, H. Zeng, Z.Chen, R. D. Little and C. Ma, *J. Electroanal. Chem.*, 751 (2015) 105.
21. Y. Zhu, Z. Chen, J. Zhang, Q. Wu, C. Ma and R. D. Little, *Electrochim. Acta*, 207 (2016) 308.
22. M. Liu, R. Zhang and W. Chen, *Chem. Rev.*, 114 (2014) 5117.
23. S. Eris, Z. Daşdelen and F. Sen, *J. Colloid Inter. Sci.*, 513 (2018) 767.
24. B. Celik, S. Kuzu, E. Erken, H. Sert, Y. Koskun and F. Sen, *Int. J. Hydrogen Energy*, 41 (2016)

3093.
25. E. Erken, H. Pamuk, O. Karatepe, G. Baskaya, H. Sert, O.M. Kalfa and F. Sen, *J. Cluster Sci.*, 27 (2016) 9.
26. D. Villers, S.H. Sun, A.M. Serventi and J. P. Dodelet, *J. Phys. Chem. B*, 110 (2006) 25916.
27. D. Bejan and A. Savall, *J. Electroanal. Chem.*, 507 (2001) 234.
28. E. Lodowicks and F. Beck, *J. Appl. Electrochem.*, 28 (1998) 873.
29. T. Tzedakis, A. Savall, *J. Appl. Electrochem.*, 27 (1997) 589.
30. C. Xiao, Q. Zou and Y. Tang, *Electrochim. Acta*, 43 (2014) 10.